



HAL
open science

Finite element modeling of nickel oxide film for Au-Ni contact of MEMS switches

Hong Liu, Dimitri Leray, Stéphane Colin, Patrick Pons

► **To cite this version:**

Hong Liu, Dimitri Leray, Stéphane Colin, Patrick Pons. Finite element modeling of nickel oxide film for Au-Ni contact of MEMS switches. 61st IEEE Holm Conference on Electrical Contacts, Oct 2015, San Diego, United States. hal-01237433

HAL Id: hal-01237433

<https://hal.science/hal-01237433>

Submitted on 3 Dec 2015

HAL is a multi-disciplinary open access archive for the deposit and dissemination of scientific research documents, whether they are published or not. The documents may come from teaching and research institutions in France or abroad, or from public or private research centers.

L'archive ouverte pluridisciplinaire **HAL**, est destinée au dépôt et à la diffusion de documents scientifiques de niveau recherche, publiés ou non, émanant des établissements d'enseignement et de recherche français ou étrangers, des laboratoires publics ou privés.

Finite element modeling of nickel oxide film for Au-Ni contact of MEMS switches

Hong Liu¹, Dimitri Leray², Stéphane Colin², Patrick Pons³

¹University of Southampton Malaysia Campus, Johor, Malaysia

²INSA-Toulouse, Toulouse, France

³LAAS, CNRS, Toulouse, France

h1v13@sotom.ac.uk

Abstract—Contamination and oxidation are inevitable in contact surfaces, especially for micro contact under low load (μN - mN). They are considered as major causes for a high contact resistance, and can lead to the failure of a contact. However, as the film formation is complicated, also it is difficult to accurately observe and measure them, the characterization of the films is not well known. In the paper, a finite element model of nickel oxide film is developed for Au-Ni contact of MEMS switches. Considering the fact that the electrical contact area is only a portion of the mechanical contact area, a model featured ‘nanospots’ is developed: multiple small conductive spots are scattered in a big mechanical contact asperity, and ultrathin oxide film is around the nanospots. The size of electrical spots and mechanical asperity is calculated based on the measured electrical resistance and mechanical contact modeling respectively. The simulation results show a good match with the experimental results. This model allows us to determine some possible geometry configuration that leads to the measured contact resistance in real devices.

Keywords—MEMS switches; electrical contact; oxide film; finite element modeling

I. INTRODUCTION

The roughness of contact surfaces plays an important role for the performance of electrical contact. For MEMS switches, the contact force is very low (μN - mN), which brings only highest asperities in contact [1], and the real contact area A_r is only a very small portion of the apparent area A_a , as $A_r = 10^{-1} - 10^{-4}A_a$ [2].

The contact resistance, or constriction resistance, can be calculated according to the ratio between contact radius and the mean free path of electrons. Three electron transport regimes were defined: diffusive, ballistic and quasi-ballistic [3], and formula were defined correspondingly [4-6].

However, it is inevitable that insulating films are formed on contact surfaces, due to oxidation, contamination, or corrosion, which prevents the current flow and cause a high resistance [7]. The electrical contact area is smaller than the physical contact area. Fig. 1 illustrates three contact areas, in which the apparent area is also called the nominal contact area, and the bearing area is to support the mechanical load, and the electrical current passes only through the electrical contact area.

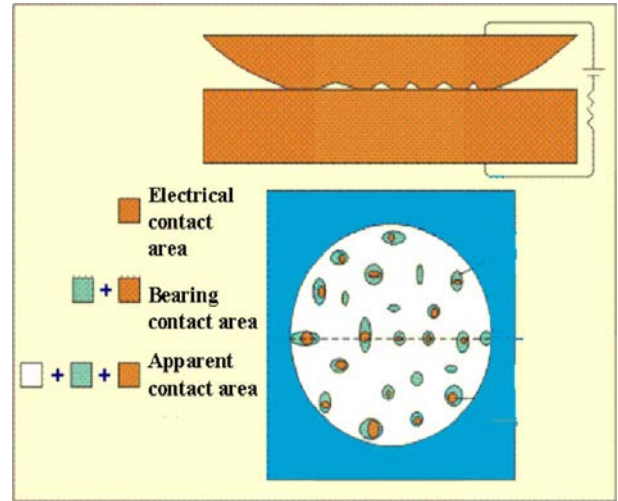


Fig. 1. Three different areas in real contact (after [8]).

The insulating films on the contact surfaces are considered as a major cause for a high contact resistance, and can lead to the failure of a contact. The composition and formation of film is complicated and would change during switching as a result of impacting and current flow. Also, it is difficult to accurately observe and measure them, the characterization of the films is not well known. Analytical calculation and numerical modeling are the alternatives.

For surfaces with insulating film resided, one simple assumption in the literature was considering the film resistance in series with the contact resistance, and the total resistance could be calculated with:

$$R_t = R_c + R_f \quad (1)$$

Where t , c , f represent the total resistance, contact resistance and film resistance.

It was shown that if the oxide film is thin enough, the electrons can pass through the film by tunnel effect, and Holm [4] suggested that the total resistance can be calculated by:

$$R_t = \rho / 2a + \sigma_f / \pi a^2 \quad (2)$$

Where ρ is the electrical resistivity of the contact material, and a is the contact radius; σ_t is the resistivity from tunnel effect, called tunnel resistivity, and is the resistance per m^2 of the surface.

Nakamura and Minowa [9, 10] used a computer simulation based on finite element model and Monte Carlo method to investigate the conduct resistance of a contact interface. The model was composed of two tubes and a random interface between the cubes. The interface was divided into a matrix of square section N^2 spots; each spot was either conductive or insulating, which was randomly selected. It was found that the conductance kept high until the fraction of the contact area was near to zero, at the moment the current density became very high and the augmentation of the conductance depended a lot the distribution and the spaces between spots.

Kogut [7, 11] presented an electrical theory for conductive and rough fractal surfaces separated by a thin insulating film, and for degraded surface, where the metallic conductance area was only a fraction of the contact area. It was found that, for a thin film, thickness < 5 nm, where the tunnel effect can occur,

- If the film covered over whole surface uniformly, then the constriction resistance was negligible compared to the resistance from tunnel effect. The total contact resistance was about 10^5 - 10^6 higher than that of clean surface [7].
- If the film was damaged, the tunnel effect became very weak compared to that of an intact film, and the I-V curves kept Ohmic [11].

It was noticed that the ballistic charge transport mechanism was dominated in Kogut's modeling, whereas it was supposed that all contact spots were in diffusive mode in Nakamura's work.

The idea of degraded films was also considered in [12, 13], where the amount of oxide film significantly impacted constriction resistance [12] because it prevented metal-to-metal contact [13]. However, no related research has been done for the case of electrical contact of MEMS switches, and there was a lack of comparison between analytical or numerical models to the experimental results in Kogut's work.

In this study, finite element models of Au-Ni contacts covered with oxide films were developed and the simulated resistance was found to be consistent with the experimental results.

II. FINITE ELEMENT MODELING

A. Contact asperity modeling

The contact asperity, which is assumed to support the mechanical load, is modeled as a 3-dimensional cone-truncated asperity as in previous study [14]. Three parameters were extracted from AFM scanning data and defined as: top radius (a), height (h) and the angle of the side with respect to the surface plan (α), as shown in Fig. 2.

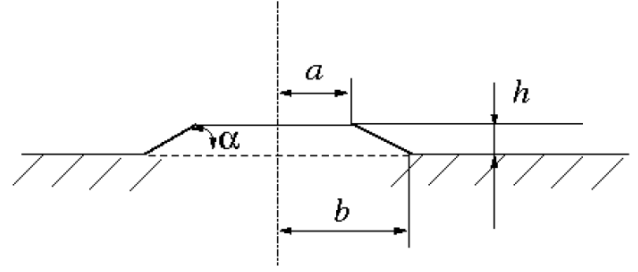


Fig. 2. Illustration of an asperity in cone-truncated geometry.

It was shown that the top radius of asperity had most significant impact on the electrical resistance and thermoelectrical behavior, whereas the height and angle only had observable influence at large values [14]. For the contact surfaces investigated in the study, which are sputtering Au-Ni, the influence of angle and height are ignored.

The top radius of the asperity (a) is defined as 120 nm in the modeling, which is based on the finite element mechanical contact modeling [15], with the applied contact force of 150 μ N, accordance to the experimental results [16]. And the height of the asperity is defined as $h=6$ nm and the angle of side as $\alpha=10^\circ$ from the AFM data [14].

B. Assumptions of insulating film

The distribution of insulating film is unknown, and two assumptions are made to take account of the residence of insulating film on the contact surface.

- Model I: The intact film, where the contact area is covered by a thin insulating film completely.
- Model II: The 'nano-spots' spots. The metallic contact spots are scattered in the oxide film, or to say, the insulating film is damaged by the metallic spots. The size of metallic spots is in order of nano meters, so called 'nano-spots' in the paper.

The schemas of the two models are shown in Fig. 3 and Fig. 4. It should be kept into mind that the dimension is not to scale in the figures, and the size of the model is given in next section.

Holm [4] indicated that an oxide film of a few atoms thick could be formed on contact surfaces after several hours exposing to the ambient environment. The crystalline parameter of NiO, the main oxide for the Au-Ni contact, is about 0.4 nm [17], so the thickness of oxide film is defined from 1 nm to 6 nm in the modeling. 6 nm is chosen as it was suggested that no tunnel effect could occur for the thickness larger than 5 nm [11].

In model II, the metallic conductive spots, are modeled as cylinders, and a few geometrical parameters are defined as:

- r_1 , the radius of nano-spots,
- h_1 , the thickness of oxide film, also the height of nano-spots,
- m_1 , the distance between two nearby nano-spots,

- n_1 , the number of nano-spots.

Simulations were performed with different values of these geometrical parameters, and a reference model is defined as:

- $r_1 = 10$ nm.
- The thickness of oxide film is $h_1 = 3$ nm.
- The number of nano-spots is $n_1 = 1$.

The radius of 10 nm is estimated with Holm equation, $R_c = (\rho_1 + \rho_2) / 4a$, with the measured contact resistance 2.55Ω at 10 mA at $150 \mu\text{N}$ [18], the calculated value is 8.9 nm, and rounded as 10 nm in the reference model. In the experiments, the contact force was applied using a nano-indentation tip on a Au-Ni MEMS switch, and the resistance was measured using the four points method [18]. Different current level was applied on the test vehicle, but only 10 mA was used in the modeling to avoid the effect of Joule heating. The influence of the geometrical parameters on electrical resistance will be discussed in section IV.

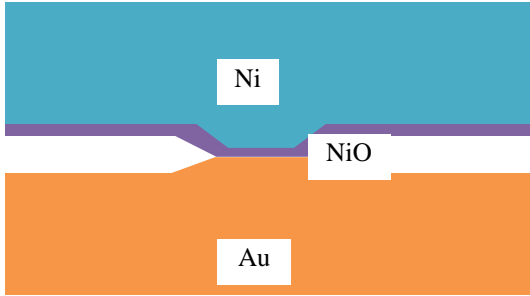
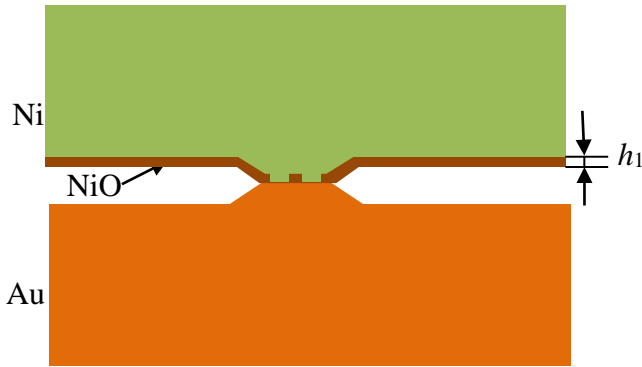
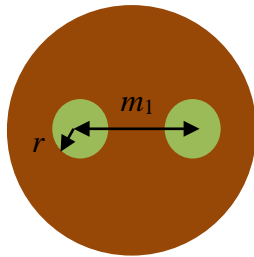


Fig. 3. Illustration of Model I: considering the contact area is covered completely by the insulating film.



(a)



(b)

Fig. 4. Illustration of Model II, called 'nano-spots', in which the insulating film is damaged by the metallic contact spots. (a) Cross section view, (b) Interface at contact area.

C. Finite element (FE) modeling

The FE model is built up with commercial software package ANSYS of version 11.0. The 3-D 10 node coupled-field element SOLID227 is used for meshing, with the degrees of freedom (DOF) of temperature and voltage activated. Fig. 5 (a) shows the meshing of the modeling and the boundary conditions. Low current of 10 mA is applied in the modeling, and the dependence of material properties on temperature is not considered in the study.

The electrical resistivity of the NiO, according to the literature [19-21], is defined in the range of 0.14×10^7 to 60×10^7 $\text{n}\Omega \times \text{m}$ in Model I, and kept as 0.3×10^7 $\text{n}\Omega \times \text{m}$ for Model II if not specified. The uncertainty of the electrical resistivity of oxide film is discussed in the last part of section IV. The material properties of the contact materials and the oxide film are listed in TABLE I.

The two contact parts are modeled as a cuboid, as shown in Fig. 5(a). The length of the cuboid is equal to the width, as $3.5 \mu\text{m}$, and the height is $1 \mu\text{m}$. The size of model has been validated to be large enough to model the constriction resistance accurately for an asperity of radius less than 200 nm.

In Model II, single nano-spot and multiple nano-spots are both modeled. For the case of one nano-spot, the spot is located at the center of underlying asperity. For multiple metallic nano-spots, the nano-spots are all of the same size, and distributed uniformly on the underlying large asperity. The thickness of oxide film is kept constant as 3 nm for multiple nano-spots modeling.

The number of nano-spots is varied in the modeling, namely as 1, 2, 4 and 9. The distance between spots is 120 nm for 2 spots and 4 spots, and is reduced to 60 nm for 9 spots due to the limited size of asperity, which has radius of 120 nm. Fig. 5 (b) shows the distribution of 9 nano-spots, and a zoom-in side view of meshing in nano-spots is shown in Fig. 5 (c).

The distribution of spots is also investigated by varying the distance between spots. The simulations were performed with 4 nano-spots of radius 10 nm, and the distance between spots were varied from 30, 60 to 120 nm.

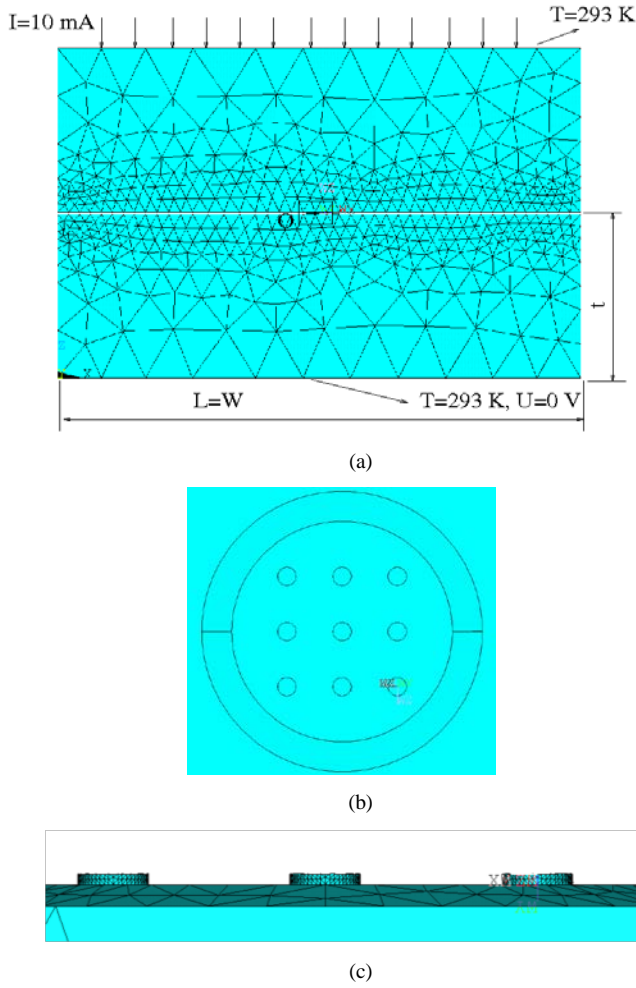


Fig. 5. (a) Meshing of the finite element model and the boundary conditions, (b) zoom in the nano-spots model, top view, (c) meshing of nano-spots, side view.

TABLE I. MATERIAL PROPERTIES FOR AU, NI AND NiO IN FEM, THE VALUES LABELED WITH * ARE FROM WIKIPEDIA WEBSITE.

Properties	Au	Ni	NiO
Electrical resistivity (nΩ×m)	22.14*	68.4*	(0.14 – 60)×10 ⁷ [19-21]
Thermal conductivity (W/(m×K))	318*	90.9*	40 [23]
Mean free path (nm)	38 [22]	9	

III. SIMPLIFIED ANALYTICAL MODEL

An analytical model is proposed to evaluate approximately the electrical resistance. It has been shown in previous study [14] that the finite element modeling could not predict the contact resistance with ballistic transport, so all the electrical resistance is calculated based on Holm equation [4]. Further more, it is assumed that:

- Tunnel effect is not taken into account, and the oxide film is considered as completely insulating;
- The electrical interaction between nano-spots is negligible;
- The supplementary electrical resistance of each nano-spot is the same as the resistance of a cylinder of height h_1 and radius r_1 , i.e. $R_{spot} = \frac{\rho_{Ni} h_1}{\pi r_1^2}$.

Thus the electrical resistance from nano-spots can be evaluated with:

$$R_{nano} = \frac{1}{n_1} \frac{\rho_{Au} + \rho_{Ni}}{4r_1} + \frac{1}{n_1} \frac{\rho_{Ni} h_1}{\pi r_1^2} \quad \square 3 \square$$

The calculation with (3) will be compared with the numerical simulations.

IV. RESULTS AND DISCUSSIONS

A. Results with Model I

The simulations were performed with the thickness of oxide film of 1 nm. The simulated total resistance is ranged from 26 Ω to 11300 Ω for the electrical resistivity of NiO varied from 0.14×10⁷ to 60×10⁷ nΩ×m, which is much larger than the measured contact resistance, 2.55 Ω. The constriction resistance of pure Au-Ni contact is only 0.18 Ω, which suggests that the resistance of oxide film dominates in the total electrical resistance.

It is concluded that in Model I, assuming the contact area is covered completely by the oxide film, the electrical resistance is too high even the film is very thin, which agrees with the results in [7]. Model I does not allow us to get the resistance close to the measured values.

B. Results with Model II

1) One nano-spot

The first investigated parameter is the radius of nano-spot. It is varied from 5 to 20 nm in the modeling, with the thickness of the oxide film kept as 3 nm. Fig. 6 shows the influence of the radius of nano-spots on the electrical resistance, compared with analytical calculation results. As expected, the resistance decreases with the radius of nano-spots increases. The analytical results compare well with the simulated values, and the maximum relative difference is only 1.8%. It is also noticed that the nano-spot of radius 10 nm results in the electrical resistance of 2.96 Ω, which is close to the measured contact resistance of 2.55 Ω [18].

The simulation was then performed with the radius of nano-spot kept as 10 nm, and the thickness of the oxide film varied from 1.5 nm to 6 nm. 1.5 nm was used in the modeling due to the meshing problem with 1 nm. The results with different thicknesses of oxide film are plotted in Fig. 7. It is shown that the thickness of oxide film does not have significant impact as the radius of nano-spots, and the total resistance increases 38% with the thickness of the film

increases from 1.5 nm to 6 nm. The difference between the analytical calculation and the FE model also increases a little bit with thicker oxide film.

It can be deduced that, with one conductive nano-spot on asperity surface, the analytical model can predict the FEM results correctly. The nano-spot with radius of 10 nm, and height of 1.5 nm or 3 nm results in the total resistance of 2.96 Ω or 2.58 Ω , which is close to the measured resistance of 2.55 Ω .

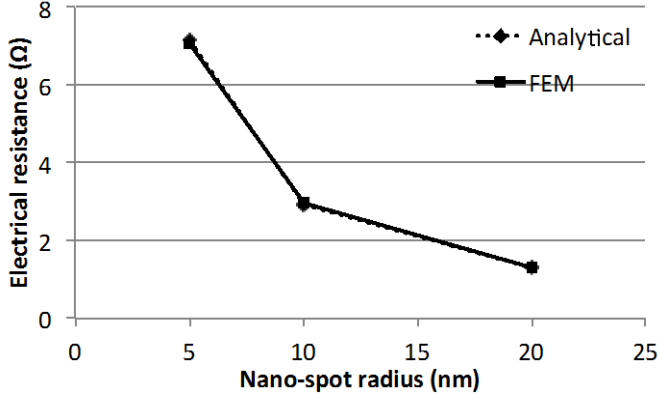


Fig. 6. Simulation results of electrical resistance as a function of nano-spot radius.

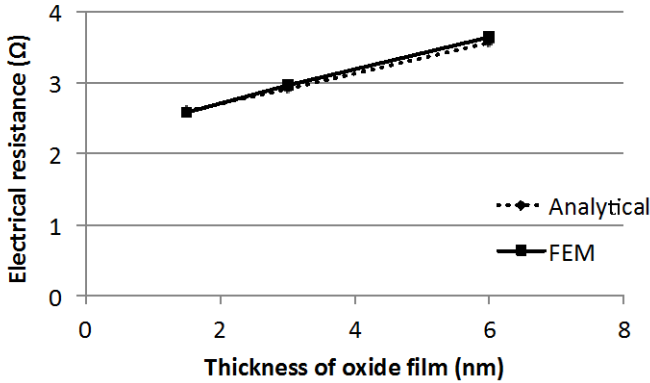


Fig. 7. Simulation results of electrical resistance as a function of oxide film thickness.

2) Multiple nano-spots

For the case of multiple nano-spots in electrical contact, the number of spots is investigated, and two radii of spots are modeled, namely as 10 nm and 5 nm.

As shown in Fig. 8, the electrical resistance decreases as the number of spots increases. This is expected as the metallic area increases with more spots, which facilitates the current flow. The electrical resistance decreases more sharply with smaller nano-spots, and the resistances tend to become stable with more spots in both cases. Due to the electrical interaction between nano-spots, the analytical calculations underestimate the electrical resistance, and the gaps between analytical calculations and FEM become bigger with the number of nano-spots increases. The relative difference with nano-spot of 10 nm is two times of that of 5 nm, and it can be deduced that the

interaction between larger nano-spots is more significant as they are closer.

It is also noticed that, the electrical resistance of 4 or 2 nano-spots of radius 5 nm, which are 1.90 Ω and 3.66 Ω , respectively, are close to the measured value of 2.55 Ω [18].

The influence of the distance between nano-spots is plotted in Fig. 9. Due to the electrical interaction between nano-spots, the electrical resistance increases when the spots are closer, and the difference between FEM and analytical model becomes bigger.

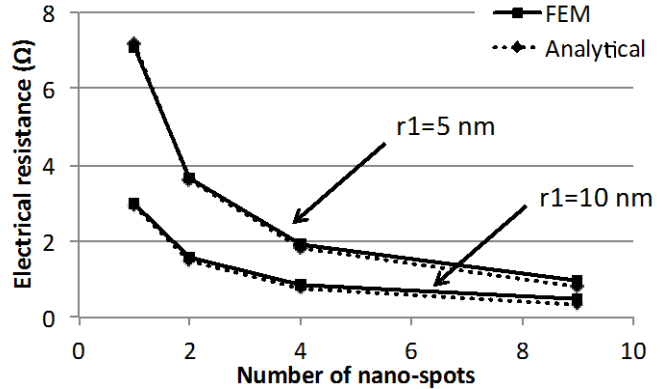


Fig. 8. Simulation results of electrical resistance as a function of number of nano-spots.

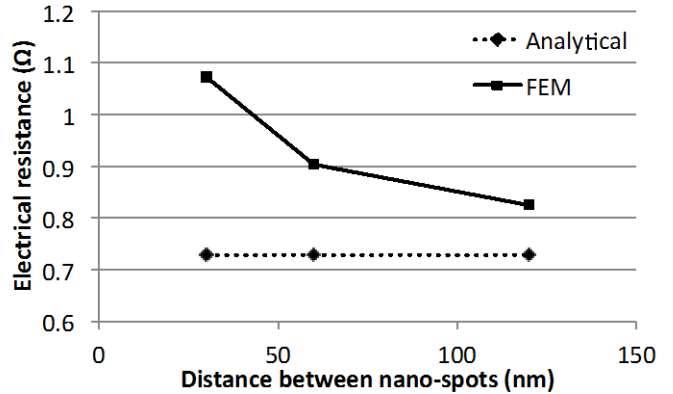


Fig. 9. Simulation results of electrical resistance as a function of distance between nano-spots. The simulations are with 4 nano-spots.

3) The influence of electrical resistivity of oxide film

The electrical resistivity of nickel oxide film is defined as 3×10^6 $n\Omega \times m$ in previous sections, which is chosen based on the values in the literature: $(0.14-60) \times 10^7$ ($n\Omega \times m$) [19-21]. These values were measured with samples fabricated in controlled conditions, either thermal evaporation or sputtering, and might be different from the natural formed oxide film. Despite the uncertainty on the resistivity value of NiO, it is noticed that the ratio of electrical resistivity between NiO and nickel is at least 20000, which suggests that the oxide film probably can be considered insulating. However, there are also some materials, like ruthenium, the oxide film is not very insulating. The electrical resistivity of Ru oxide film is only 5 times bigger than that of ruthenium (with $\rho_{Ru} = 76$ ($n\Omega \times m$), and $\rho_{RuO_2} = 350$ ($n\Omega \times m$) [24]. In this section, the influence of

electrical resistivity of oxide film on the total electrical resistance is discussed, and a new analytical model is proposed.

The simulation is performed with one conductive nano-spot on asperity surface. The radius of nano-spot is 10 nm, and the thickness of oxide film is 3 nm. The minimum value of electrical resistivity of oxide film is defined as about 1/20 of the value in the literature, which is about 1/1000 of the electrical resistivity of nickel. The range of electrical resistivity of oxide film is varied then from 7.5×10^4 to 60×10^7 ($n\Omega \times m$) in the modeling.

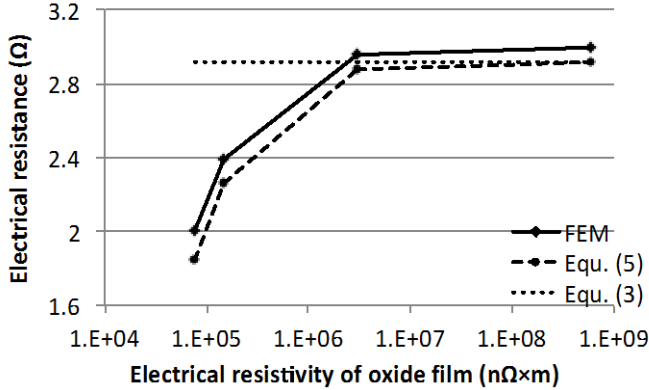


Fig. 10. Simulation results of electrical resistance as a function of number of nano-spots.

The simulated total resistance is plotted in Fig. 10, and it is found that the total electrical resistance drops significantly with the electrical resistivity of NiO decreases from 3×10^6 ($n\Omega \times m$) to 0.15×10^6 ($n\Omega \times m$), this indicates that the conductance of oxide film is not negligible when its electrical resistivity is small, here about 1/2000 of that of nickel.

We assume the electrical resistance from the oxide film laying on the asperity can be evaluated by the bulk resistance formula ($R = \rho \times l / A$), as:

$$R_{nlm} = \rho_{NiO} \frac{h_1}{\pi(a^2 - r_1^2)} \quad (4)$$

The total contact resistance then can be evaluated considering the electrical resistance from oxide film (4) and the resistance from nano-spots (3) in parallel, and we have:

$$R_{total} = \left(\frac{1}{R_{nano}} + \frac{1}{R_{nlm}} \right)^{-1} \quad (5)$$

$$= \left[\left(\frac{\rho_{Ni} + \rho_{Au}}{4r_1} + \rho_{Ni} \frac{h_1}{\pi r_1^2} \right)^{-1} + \left(\rho_{NiO} \frac{h_1}{\pi(a^2 - r_1^2)} \right)^{-1} \right]^{-1}$$

The total contact resistance calculated using (5) is also plotted in Fig. 10, compared with the ones using (3). It is found that the new analytical model can predict the contact resistance more accurately for the oxide film with low electrical resistivity. It is also noticed that when the R_{nano} is close to the R_{total} , the oxide film can be considered as completely insulating. For the oxide film with very low electrical

resistivity, like RuO₂, the results would be much different from the Au-Ni contact discussed in the study.

V. CONCLUSIONS

A finite element model was developed for the oxide film of Au-Ni contact. Two types of insulating film are investigated: intact and damaged. A ‘nano-spots’ model is built up for the damaged insulating film. The metallic conductive spots are scattered in the oxide film that is laid on a mechanical contact asperity. The size of mechanical asperity is calculated from the FE contact modeling, and that of nano-spots are evaluated from the measured resistance. The size of nano-spots and thickness of oxide films are investigated, also the number and distribution of nano-spots for the case of multiple metallic spots.

Two simplified analytical models are proposed, and the influence of electrical resistivity of oxide film is discussed. It is shown that the oxide film cannot be considered insulating when the electrical resistivity is about 1/2000 of that of the metal, and the improved analytical model is more accurate for this case.

It is found that one nano-spot with radius of 10 nm or 4 or 2 nano-spots with radius of 5 nm produce the electrical resistance close to the measured results. The FE model and analytical model shed light on the possible geometry configuration of insulating film on the contact surfaces. It should also be kept in mind that the ballistic transport is not considered in the study.

REFERENCES

- [1] B. F. Toler, R. A. Coutu, and J. W. McBride, “A review of micro-contact physics for microelectromechanical systems (MEMS) metal contact switches,” *J. Micromechanics Microengineering*, vol. 23, no. 10, p. 103001, Oct. 2013.
- [2] K.-H. Grote and E. K. Antonsson, *Springer Handbook of Mechanical Engineering*. Springer Science & Business Media, 2009.
- [3] N. Agraït, A. L. Yeyati, and J. M. van Ruitenbeek, “Quantum properties of atomic-sized conductors,” *Phys. Rep.*, vol. 377, no. 2–3, pp. 81–279, avril 2003.
- [4] R. Holm, *Electric Contacts-Theory and Applications, 4th edn.* Berlin: Springer, 1967.
- [5] Y. V. Sharvin, “A Possible Method for Studying Fermi Surfaces,” *Sov. Phys. JETP*, vol. 21, p. 655, 1965.
- [6] G. Wexler, “The size effect and the non-local Boltzmann transport equation in orifice and disk geometry,” *Proc Phys Soc*, vol. 89, pp. 927–941, 1966.
- [7] L. Kogut and K. Komvopoulos, “Electrical contact resistance theory for conductive rough surfaces separated by a thin insulating film,” *J. Appl. Phys.*, vol. 95, pp. 576–585, 2004.
- [8] A. Monnier, B. Froidurot, C. Jarrige, P. Testé, and R. Meyer, “A Mechanical, Electrical, Thermal Coupled-Field Simulation of a Sphere-Plane Electrical Contact,” *IEEE Trans. Compon. Packag. Technol.*, vol. 30, pp. 787–795, 2007.
- [9] M. Nakamura and I. Minowa, “Computer Simulation for the Conductance of a Contact Interface,” *IEEE Trans. Compon. Hybrids Manuf. Technol.*, vol. 9, no. 2, pp. 150–155, 1986.
- [10] M. Nakamura and I. Minowa, “Film resistance and constriction effect of current in a contact interface,” *IEEE Trans. Compon. Hybrids Manuf. Technol.*, vol. 12, no. 1, pp. 109–113, Mar. 1989.
- [11] L. Kogut, “Electrical performance of contaminated rough surfaces in contact,” *J. Appl. Phys.*, vol. 97, pp. 103723–1–103723–5, 2005.
- [12] T. Hisakado, “Effects of surface roughness and surface films on contact resistance,” *Wear*, vol. 44, no. 2, pp. 345–359, Sep. 1977.

- [13] E. Crinon and J. T. Evans, "The effect of surface roughness, oxide film thickness and interfacial sliding on the electrical contact resistance of aluminium," *Mater. Sci. Eng. A*, vol. 242, no. 1–2, pp. 121–128, Feb. 1998.
- [14] H. Liu, D. Leray, P. Pons, and S. Colin, "An Asperity-Based Finite Element Model for Electrical Contact of Microswitches," in *Holm Conference on Electrical Contacts (HOLM)*, 2013 IEEE 59th, Newport, RI, USA, 2013, pp. 1–10.
- [15] H. Liu, D. Leray, S. Colin, P. Pons, and A. Broué, "Finite Element Based Surface Roughness Study for Ohmic Contact of Microswitches," in *58th IEEE Holm Conference on Electrical Contacts (Holm)*, Portland, OR, 2012, pp. 1–10.
- [16] A. Broué, J. Dhennin, P. Charvet, P. Pons, N. B. Jemaa, P. Heeb, F. Coccetti, and R. Plana, "Multi-Physical Characterization of Micro-Contact Materials for MEMS Switches," in *Proceedings of the 56th IEEE Holm Conference on Electrical Contacts*, Charleston, SC, 2010, pp. 1–10.
- [17] I. Hotový, D. Búč, Š. Haščík, and O. Nennowitz, "Characterization of NiO thin films deposited by reactive sputtering," *Vacuum*, vol. 50, no. 1–2, pp. 41–44, mai 1998.
- [18] A. Broué, "Analyse multi physique des sources de défabilisation du microcontact électrique à destination des interrupteurs MEMS," Univ de Toulouse, 2012.
- [19] Y. M. Lu, W. S. Hwang, J. S. Yang, and H. C. Chuang, "Properties of nickel oxide thin films deposited by RF reactive magnetron sputtering," *Thin Solid Films*, vol. 420–421, pp. 54–61, 2002.
- [20] G. Wakefield, P. J. Dobson, Y. Y. Foo, A. Loni, A. Simons, and J. L. Hutchison, "The fabrication and characterization of nickel oxide films and their application as contacts to polymer/porous silicon electroluminescent devices," *Semicond Sci Technol*, vol. 12, pp. 1304–1309, 1997.
- [21] H. Sato, T. Minami, S. Takata, and T. Yamada, "Transparent conducting p-type NiO thin films prepared by magnetron sputtering," *Thin Solid Films*, vol. 236, pp. 27–31, 1993.
- [22] R. S. Timsit, "Electrical Conduction Through Small Contact Spots," *Trans. Compon. Packag. Technol.*, vol. 29, pp. 727–734, 2006.
- [23] F. B. Lewis and N. H. Saunders, "The thermal conductivity of NiO and CoO at the Neel temperature," *J Phys C Solid State Phys*, vol. 6, pp. 2525–2532, 1973.
- [24] R. M. Hawk, K. V. Gadepally, and D. N. Patangia, "Properties of ruthenium oxide coatings," *Proc. Ark. Acad. Sci.*, vol. 45, 1991.